ILMATIETEEN LAITOS
METEOROLOGISKA INSTITUTET
FINNISH METEOROLOGICAL INSTITUTE

RAPORTTEJA
RAPPORTER
REPORTS
2006:9

Climate Projections for the Nordic CE Project - An Analysis of an Extended set of Global and Regional Climate Model Runs

KIMMO RUOSTEENOJA
KIRSTI JYLHÄ
PETRI RÄISÄNEN

RAPORTTEJA
RAPPORTER
REPORTS
No. 2006:9

551.588.74
551.524.34
551.577.34

CLIMATE PROJECTIONS FOR THE NORDIC CE PROJECT — AN ANALYSIS OF AN EXTENDED SET OF GLOBAL AND REGIONAL CLIMATE MODEL RUNS

Kimmo Ruosteenoja
Kirsti Jylhä
Petri Räisänen

Ilmatieteen laitos
Meteorologiska Institutet
Finnish Meteorological Institute

Helsinki 2006

ISBN 951-697-659-X
ISSN 0782-6079 (Raportteja – Rapporter – Reports)

Yliopistopaino
Helsinki 2006

FINNISH METEOROLOGICAL INSTITUTE

Published by Finnish Meteorological Institute
(Erik Palménin aukio 1) , P.O. Box 503
FIN-00101 Helsinki, Finland

Series title, number and report code of publication
Reports No. 2006:9

Date 2006

Authors
Kimmo Ruosteenoja, Kirsti Jylhä, Petri Räisänen

Name of project
Nordic Project on Climate and Energy

Commissioned by
Nordic Energy Research (NEFP)

Title
CLIMATE PROJECTIONS FOR THE NORDIC CE PROJECT - AN ANALYSIS OF AN EXTENDED SET OF GLOBAL AND REGIONAL CLIMATE MODEL RUNS

Abstract
The regional 'production' climate scenarios provided for the Nordic Project on Climate and Energy (CE) project were based on dynamical downscaling of two global climate models (GCMs), merely considering two SRES emission scenarios. To better meet the full uncertainty of future climate evolution, an extended set of climate projections was constructed. Mean temperature and precipitation projections were composed for two 30-year periods for seven regions covering Northern Europe and Greenland. Projections were formulated for the A1FI, A2, B2 and B1 scenarios, employing the super-ensemble pattern scaling method when a model response to some forcing scenario was not available.

The median estimates based on projections by six GCMs or, alternatively, by ten regional climate models (RCMs) within the EU-funded PRUDENCE project, were almost invariably statistically significant for temperature change, but less frequently so for precipitation, especially in summer. In Greenland by 2070-2099, however, precipitation was projected to increase significantly in all seasons.

The temperature changes in the CE 'production' climate simulations generally fell inside the 95% probability intervals of a Gaussian fit to the GCM-based projections. For Northern Europe, however, the HadAM3H-driven CE A2 runs produced weaker wintertime warming than the GCMs for the same forcing scenario. Compared with the GCM estimates, CE production scenarios were generally wetter in winter and drier in summer.

Annual numbers of frost and snow cover days in northern Europe decreased by about 30%, in Baltic countries even more, but there was a large scatter among the projections by individual RCMs. One-day maximum precipitation tends to increase in most cases, even so in summer, when changes in mean precipitation are quite small - an indication of a more extreme summertime precipitation climate in the future.

Publishing unit Climate and Global Change

Classification (UDK)
551.588.74, 551.524.34, 551.577.34

Keywords
Mean temperature projections; Precipitation projections; Global climate models; Regional climate models; Northern Europe; Frost days; Snow cover days; Maximum one-day precipitation; SRES scenarios

ISSN and series title 0782 – 6079 Raportteja – Rapporter - Reports

ISBN
951-697-659-X

Language
English

Sold by
Finnish Meteorological Institute / Library
P.O.Box 503, FIN-00101 Helsinki
Finland

Pages 28

Price

Note

ILMATIETEEN LAITOS

Julkaisun sarja, numero ja raporttikoodi
Raportteja No. 2006:9

Julkaisija Ilmatieteen laitos, (Erik Palménin aukio 1)
PL 503, 00101 Helsinki

Julkaisuaika 2006

Tekijä(t)
Kimmo Ruosteenoja, Kirsti Jylhä, Petri Räisänen

Projektin nimi
Nordic Project on Climate and Energy
Toimeksiantaja Nordic Energy Research (NEFP)

Nimeke

LAAJAAN ILMASTOMALLIAINEISTOON PERUSTUVIA ILMASTONMUUTOSENNUSTEITA POHJOISMAISELLE ILMASTO JA ENERGIA -TUTKIMUSHANKKEELLE

Tiivistelmä

Pohjoismaisen Ilmasto ja energia -tutkimushankkeen (CE-hanke) tuottamat ilmastonmuutoksen ns. perusennusteet pohjautuivat kahdella alueellisella ilmastomallilla tehtyihin kokeisiin. Näissä kokeissa tarkasteltiin ainoastaan kahta SRES-skenaariota, ja malliajoissa käytetyt reunaehdot oli otettu vain kahdesta maailmanlaajuisesta mallista. Ilmastoennusteitten todellisen epävarmuushaarukan selvittämiseksi tässä tutkimuksessa tarkasteltiin paljon useampia malleja. Ilmastoennusteet laskettiin 30-vuotisjaksoille 2021-50 ja 2070-99, erikseen seitsemälle maantieteelliselle alueelle, jotka yhdessä kattoivat Pohjois-Euroopan ja Grönlannin. Ennusteet laadittiin erikseen A1FI-, A2-, B1- ja B2-skenaarioille. Useimmista malleista ei ollut käytettävissä simulaatiota kaikille näille skenaariolle, ja tällöin puuttuvat arvot saatiin skaalaamalla olemassa olevien ajojen tuloksia. Skaalauksessa laskettiin kaikista yksittäisen mallin skenaarioajoista lineaarinen regressioyhtälö kuvaamaan ilmastosuureen alueellisen muutoksen ja maapallon keskilämpötilan muutoksen välistä yhteyttä.

Malliajojen keskiarvoina saadut lämpötilan muutokset olivat lähes poikkeuksetta tilastollisesti merkitseviä. Tämä koski sekä kuuden maailmanlaajuisen että kymmenen alueellisen ilmastomallin antamia muutoksia. Sademäärän ennustettu muutos ei sen sijaan monissa tapauksissa ollut tilastollisesti merkitsevä, varsinkaan kesällä. Kuitenkin Grönlannissa satoi vuosisadan lopulla tilastollisesti merkitsevästi nykyisiä enemmän kaikkina vuodenaikoina.

CE-hankkeen tuottamat lämpötilan ja sademäärän muutoksen perusennusteet osuivat yleensä tässä tutkimuksessa laajemman mallijoukon perusteella saatuun 95% epävarmuushaarukkaan. Kuitenkin HadAM3H-mallia reunaehtona käyttävissä CE-hankkeen A2-skenaarioajoissa ilmaston lämpeneminen jäi heikommaksi kuin maailmanlaajuisissa malleissa. Sademäärät lisääntyivät CE-hankkeen malliajoissa talvella enemmän kuin tässä tutkimuksessa ja pysyivät kesällä lähes ennallaan.

Pakkas- ja lumipeitepäivien määrä putosi vuosisadan loppuvuosikymmenille tultaessa Pohjois-Euroopassa noin 30%, Baltian maissa enemmänkin. Eri mallien ennusteet kuitenkin poikkesivat toisistaan melkoisesti. Suurimmat vuorokautiset sademäärät yleensä kasvoivat. Näin kävi kesälläkin, vaikka tuolloin keskimääräinen sademäärä ei juuri näytä muuttuvan. Tämä osoittaa sadeolojen muuttuvan tulevaisuudessa kesäisin entistä äärevimmiksi.

Julkaisijayksikkö Ilmasto ja globaalimuutos

Luokitus (UDK) 551.588.74, 551.524.34, 551.577.34

Asiasanat
Keskilämpötilojen ennustetut muutokset; Sademäärien ennustetut muutokset; Maailmanlaajuiset ilmastomallit; Alueelliset ilmastomallit: Pohjois-Eurooppa; Pakkaspäivät; Lumipeitepäivät; Vuorokautiset maksimisademäärät; SRES-skenaariot

ISSN ja avainnimike 0782 – 6079 Raportteja – Rapporter - Reports

ISBN 951-697-659-X

Kieli Englanti

Myynti Ilmatieteen laitos / Kirjasto
PL 503, 00101 Helsinki

Sivumäärä 28

Hinta

Lisätietoja

Contents

1 Introduction

In the Nordic Project on Climate and Energy (CE)[1], the widely utilized so called Production scenarios were based on simulations performed with two regional climate models (RCMs): the Swedish RCA model and two versions of the HIRHAM model, one employed in Denmark and the other in Norway (RUMMUKAINEN, 2006). In these experiments, two alternative IPCC (2001) SRES emission scenarios and boundary data from two global climate models (GCMs) are applied. Accordingly, these simulations comprise only a small subset of possible future evolutions. DÉQUÉ et al. (2006) report that differences between the simulations arising from the driving GCM are generally larger than those due to the internal structures of RCMs.

The first purpose of the present work is to put those RCM simulations into a wider perspective by formulating near-surface (2 m) air temperature and precipitation projections that are based on experiments performed with six coupled atmosphere-ocean GCMs. These GCMs represent climate sensitivities and patterns of change that are much more variable than those in the two GCMs employed to drive the CE RCM simulations. Projections are composed, in addition to the intermediate A2 and B2 scenarios used in the CE Production scenario simulations, for two extreme scenarios, the B1 scenario representing a very low and the A1FI scenario extremely high emissions of greenhouse gases. In addition, we present some projections that are based on the large suite of RCM runs participating in the PRUDENCE project (CHRISTENSEN et al., 2006).

Projections are presented for two future 30-year time spans, 2021–2050 and 2070–2099 (for RCMs the latter period is 2071–2100), relative to the baseline period 1961–1990. All the projections are presented as domain averages for a number of discrete regions of subcontinental or smaller scale, together covering the CE study domain. Six of these regions (see acronyms in the caption) are depicted in Fig. 1. In addition, projections are composed for the large Northern Europe continental region (“NEU”) that is a combination of regions “SCA”, “FEN” and “BAL”.

For each regional projection, both the mean estimate and a 95% probability interval will be reported. The statistical significance of the projections is assessed by comparing the mean estimate with a measure of internal variability of the climate system, derived from millennial unforced simulations performed with two GCMs.

The B1- and A1FI-forced simulations are not available for most of the six GCMs. Thus pattern scaling from the existing simulations has to be employed to compose projections corresponding to these forcing scenarios. Analogously, for the PRUDENCE RCMs, projections for the

[1] http://www.os.is/ce/

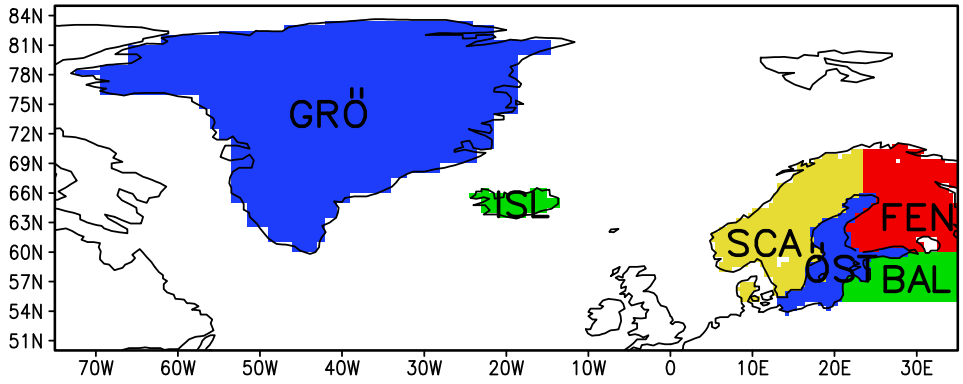

Fig. 1. Regional subdivision applied to represent the GCM- and RCM-based climate projections. GRÖ = Greenland, ISL = Iceland, SCA = Scandinavia, FEN = Fennoscandia, ÖST = Baltic Sea, BAL = Baltic area.

period 2021–50 are scaled from the simulations for 2071–2100.

In several applications of climate data, information about changes in the mean state is not adequate. Therefore various indices related to frost, snow and heavy precipitation etc. have been developed. In this account, changes in several relevant climate indices from the baseline period to the time span 2071–2100 have been derived from the suite of RCM A2 and B2 simulations. The relationship between those indices and mean temperature and precipitation is not necessarily linear. Therefore no attempt has been made to scale these indices to the extreme SRES scenarios or to the first scenario period.

The methodology employed to construct the climate projections is presented in section 2. Many of these tools have been developed to be used jointly in the PRUDENCE and CE projects; in those cases, details reported in our PRUDENCE papers (RUOSTEENOJA et al., 2006, hereafter referred to RJT06; JYLHÄ et al., 2006) are not repeated here. A brief analysis of the probabilistic mean temperature and precipitation projections is given in section 3, while changes in the climate indices are discussed in section 4. Tables including a complete set of regional mean temperature and precipitation projections are presented in the Appendix of this report.

2 Methodology

2.1 Models analyzed

Information about the GCMs and the runs performed is given in Table 1. Further details and references to model documentation can be found in MCAVANEY et al. (2001). The

responses to the A2 and B2 forcing scenarios have been simulated with all GCMs. The low-forcing B1 response was available for HadCM3 and CSIRO Mk2, while the high-forcing A1FI response was only available for HadCM3. Furthermore, HadCM3 was the only model for which ensemble runs were available, the ensemble size being 3 runs for the A2 and 2 runs for the B2 scenario[2].

The RCM runs analyzed in this study are listed in Table 2. Most RCMs contain an atmospheric component only (in two RCMs a submodel for the Baltic Sea was utilized), the sea surface data and atmospheric lateral boundary values being derived from a global GCM. Experiments driven by the HadCM3/HadAM3 modelling system have been conducted with all the RCMs, but there are only two models (HIRHAM (dk) and RCAO) for which ECHAM4/OPYC3-forced runs are available. Arpège/OPA has been employed as a driving model by one RCM only. All models have been used to calculate the response to the A2 forcing, while B2 runs are available for a minority of them.

2.2 Super-ensemble pattern-scaling to construct B1 and A1FI projections

Except for two GCMs out of six, only responses to the SRES A2 and B2 forcing scenarios have been simulated (see Table 1). In order to formulate projections for the highest (A1FI) and lowest (B1) scenarios, a super-ensemble pattern-scaling technique has been developed. This method uses linear regression to represent the relationship between the local GCM-simulated temperature/precipitation response and the global mean temperature change simulated by the simple MAGICC climate model (RAPER et al., 2001). For a detailed description and an performance analysis of the method, the reader is referred to RJT06.

2.3 Pattern-scaling with respect to time

Apart from the transient ECHAM4-forced simulations by RCAO, no RCM-simulated data are available in the CE project for time spans earlier than 2070. Therefore, in order to compose RCM-based temperature and precipitation projections for earlier periods, responses calculated for the periods 2070–2099 or 2071–2100 must be scaled in time.

Temporal scaling is based on the simple approach proposed by CHRISTENSEN et al. (2001):

$$\Delta X(t) = \alpha \Delta X(t_0) \tag{1}$$

[2]In contrast to some earlier work plans of the CE project, we have included these HadCM3 parallel runs in our analysis instead of HadAM3; HadAM3 is not a coupled GCM since there is no oceanic component.

Table 1. Coupled GCMs analyzed for the CE project. Column 1 gives the model acronym and column 2 the country where the model was developed. To illustrate the model resolution, the horizontal grid distance in the north-south $\times$ east-west direction (GRID) and the number of model levels in the vertical (L) are given. The last column gives the SRES scenarios for which runs were performed.

MODEL	COUNTRY	GRID	L	SCENARIOS
CGCM2	Canada	$3.8 \times 3.8°$	10	A2, B2
CSIRO Mk2	Australia	$3.2 \times 5.6°$	9	A2, B1, B2
ECHAM4/OPYC3	Germany	$2.8 \times 2.8°$	19	A2, B2
GFDL R30	U.S.A.	$2.2 \times 3.8°$	14	A2, B2
HadCM3	United Kingdom	$2.5 \times 3.8°$	19	A1FI, A2, B1, B2
NCAR DOE PCM	U.S.A.	$2.8 \times 2.8°$	18	A2, B2

Table 2. The RCMs employed in this CE account, with the following characteristics defined: the model acronym (MODEL), country of origin (COUNTRY), horizontal resolution (RESOL) and the number of levels (L). The final column gives the global models which provided the driving data for the RCM run and the SRES scenarios for which experiments have been performed. For further information, see DÉQUÉ et al. (2006).

MODEL	COUNTRY	RESOL	L	DRIVING MODELS (SCENARIOS)
HIRHAM (dk)	Denmark	49 km	19	HadCM3/HadAM3H (A2), ECHAM4 (A2; B2)
HIRHAM (no)[1]	Norway	56 km	19	HadCM3/HadAM3H (A2; B2)
HadRM3P	Britain	49 km	19	HadCM3/HadAM3P (A2; B2)
CHRM	Switzerland	56 km	20	HadCM3/HadAM3H (A2)
CLM	Germany	56 km	20	HadCM3/HadAM3H (A2)
REMO	Germany	56 km	19	HadCM3/HadAM3H (A2)
RCAO	Sweden	49 km	24	HadCM3/HadAM3H (A2; B2), ECHAM4 (A2; B2)[2]
PROMES	Spain	50 km	28	HadCM3/HadAM3H (A2)
RACMO	Netherlands	49 km	31	HadCM3/HadAM3H (A2)
Arpège[3]	France	50 – 70 km	31	HadCM3/HadAM3H (A2; B2), Arpège/OPA (A2; B2)

[1] Norwegian HIRHAM runs (ENGEN-SKAUGEN et al., 2005) were not available for PRUDENCE, and thus that model is not included in the analysis of section 3.

[2] For ECHAM4/OPYC3, the HIRHAM (dk) and RCAO simulations employ boundary data from a different ensemble member.

[3] Arpège is actually a global model with spatially-varying grid size. The 50–70 km grid is employed over Europe.

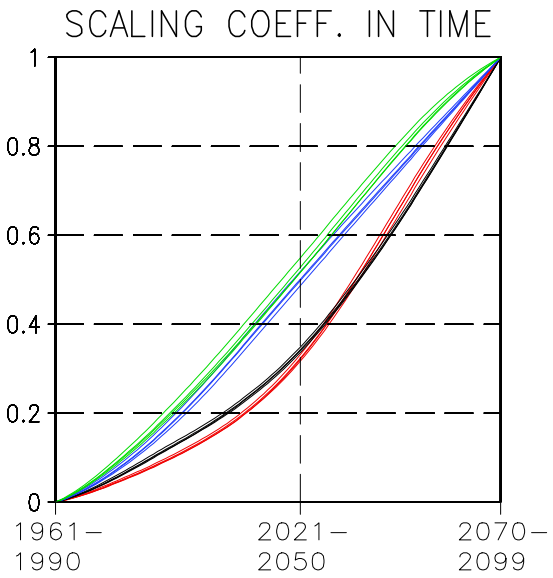

Fig. 2. Scaling coefficients employed to compose temperature and precipitation change projections for individual 30-year periods inside the interval 1961–1990 – 2070–2099, relative to the baseline period 1961–1990. Red curves display the scaling coefficients for the A1FI scenario, black, green and blue curves for the A2, B1 and B2 scenarios, respectively. Coefficients are given separately for four GCMs (HadCM3, CSIRO-Mk2, NCAR DOE PCM and ECHAM4/OPYC3); in practice, curves for the various models deviate little from one another.

where ΔX is the local or regional temperature or precipitation response relative to the baseline period 1961–1990. t_0 refers to the period 2070–2099 (or 2071–2100) and t to the tridecadal period for which the scaled response is estimated. The temporal scaling coefficient α takes the form

$$\alpha = \frac{\langle \Delta T(t) \rangle}{\langle \Delta T(t_0) \rangle} \tag{2}$$

where the global mean temperature change $\langle \Delta T \rangle$ is adopted from the MAGICC climate model (RAPER et al., 2001). Accordingly, in employing this technique we assume that the local temperature and precipitation responses are linearly proportional to the global mean temperature response.

Temporal scaling coefficients for the four GCMs for which MAGICC emulations were available are depicted in Fig. 2. Coefficients for the various GCMs are very close to one another. In both B scenarios, the temporal evolution of global mean temperature is nearly linear in time, whereas in the A scenarios warming tends to accelerate towards the end of the period.

In practice, the procedure for calculating the temporally-scaled responses is following. First, one must have ΔX for the period 2070–2099. For SRES scenarios with no RCM runs available, that response can be generated by the super-ensemble pattern-scaling method (section

2.2). Second, this temperature or precipitation response for the period 2070–2099 is multiplied by the temporal scaling coefficient (2) corresponding to the respective time span, SRES scenario and driving GCM.

In the Appendix, regional RCM temperature and precipitation responses to the A2 scenario are given for the time spans 2021–2050 (temporally scaled) and 2071–2100 (directly from the model simulation).

A disadvantage of the above procedure is that for the A2 and B2 scenarios the temporally-scaled response is determined by a single modelled pattern $\Delta X(t_0)$, which increases the proportion of noise in the scaled response. Noise might be reduced by employing the super-ensemble regression equation to construct $\Delta X(t_0)$ for these scenarios as well, but this approach may produce biased results if the relationship between the local response and the global mean temperature change is strongly nonlinear.

2.4 Construction of 95% probability intervals for regional projections

Owing to the small number of GCMs analyzed (six), the GCM projections applied as such do not give a statistically representative picture of regional climate change. Instead, we have fitted the normal (Gaussian) distribution to the set of model projections. In general, the projections appeared to follow the normal distribution fairly well (RJT06), although there are some cases in which the fit is less successful (section 3).

Utilizing the Gaussian approximation, we can construct 95% probability intervals for the temperature and precipitation change:

$$I_{j,k}^{\Delta T} = \overline{\Delta T_{j,k}} \pm 1.96 s_{j,k}^{\Delta T}; \quad I_{j,k}^{\Delta P} = \overline{\Delta P_{j,k}} \pm 1.96 s_{j,k}^{\Delta P} \tag{3}$$

where the subindices j and k refer to the seven regions and four seasons, respectively. The overbar stands for a mean over the six models, s for the standard deviation. In calculating the means and standard deviations, HadCM3 ensemble runs have been given a double total weight compared to the other GCMs.

For the RCM-based probability intervals, two versions were calculated. The first one was inferred directly from the HadCM3/HadAM3-forced RCM runs. Another version emulates an extended set of RCM runs forced by three GCMs: HadCM3, ECHAM4 and Arpège. Since, for most of the RCMs, no runs applying the two latter boundary models have been performed, the set was synthetically extended to cover these missing runs; details are explained in RJT06. In calculating the RCM temperature and precipitation responses, for the HIRHAM model we merely used the Danish version.

2.5 Comparison of climate change signal with spread due to internal variability

In order to assess the statistical significance, projected temperature and precipitation responses were compared with the magnitude of internal variability in millennial control simulations performed with HadCM3 and CGCM2. In analyzing the statistical significance of the model-simulated climate change, one needs an estimate of the internal variability on the equivalent temporal scale. Accordingly, standard deviations of temperature and precipitation were calculated from a series of 30-year temporal averages of regional-mean values. Finally, the standard deviations were multiplied by $\sqrt{2}$ to give an expectation for the *difference* between two arbitrarily-chosen 30-year means.

2.6 Computation of climatic indices

Changes in indices related to frost, snow and heavy precipitation in the Nordic mainland at the end of the 21st century were analyzed based on experiments performed with an extensive suite of RCM simulations (Table 2). In this analysis both versions of HIRHAM were included. The following indices were considered: the annual number of frost days (FD, i.e., days with a minimum air temperature $< 0°$C); the dates of the first autumnal and the last vernal frosts; maximum one-day precipitation; maximum number of consecutive dry days; the number of days with snow cover (SCD, i.e., days with the simulated snow water equivalent > 0 kg/m^2). Future changes in these indices have implications for hydropower resources and heating energy demand.

The projected changes for the period 2071–2100, compared to the baseline period 1961–1990, are given as domain averages over three sub-regions of the CE study domain (Fig. 1): “SCA”, “FEN”, and “BAL” (the computational domain of the PRUDENCE RCM simulations does not cover Iceland and Greenland). Domain-averaging enabled straightforward comparisons of the various RCM experiment, but required that the indices be interpolated onto a common geographical latitude-longitude grid. Before calculating the indices related to frost, all simulated daily minimum temperature data were adjusted to reduce the influence of differences in topography between the regular geographical grid and the native RCM grids (for details, see JYLHÄ et al., 2006).

3 Regional temperature and precipitation projections

Figures 3–4 illustrate GCM-based 95% probability intervals of temperature and precipitation change for period 2070–2099; projections are given here for three example regions, northern Europe (NEU), Iceland (ISL) and Greenland (GRÖ). Also depicted in the figures is 1.96 times the standard deviation of the difference between two arbitrarily-chosen 30-year means. This measure of internal variability is an average of the estimates given by the HadCM3 and CGCM2 control simulations. Responses outside those bars can be considered statistically significant at the 5% level.

In Fig. 3, the best estimates for the temperature change, or the medians of the probability intervals, are distinctly statistically significant, warming being stronger in winter than in summer. The six-GCM mean warming is a monotonous function of the strength of the radiative forcing, the A1FI forcing producing a warming nearly double that of B1. However, the probability intervals are quite broad, reflecting the large scatter among the various model simulations. The probability intervals representing different forcing scenarios thus overlap strongly.

The 95% probability intervals for precipitation change are presented in Fig. 4. As far as best estimates are considered, precipitation is projected to increase. In northern Europe strongest increase is projected for winter, in Greenland for summer and winter and in Iceland for intermediate seasons. Statistical significance of the precipitation change is lower than that for the temperature increase.

Calculation of the probability intervals by Eq. (3) calls for that the distribution of individual GCM responses is sufficiently close to normal. As discussed in RJT06, this approximation ordinarily holds. However, there are individual cases in which one of the GCMs yields a simulation that deviates markedly from the remaining ones, making the distribution significantly skewed. A striking example of a situation is the Iceland temperature response in winter and spring (see the second panel of Figs. 3). One anomalous model, in this case NCAR DOE PCM[3], spuriously widens the probability interval at *both* ends. Thereby the lower end of the interval becomes negative, although all individual GCMs project distinct warming. In the absence of such an outlier, the width of the interval would be reduced much, and even the lower end would be positive. Accordingly, the Gaussian distribution is not a particularly good tool for studying such a special case. Another example of that problem is the wintertime precipitation change in northern Europe, where ECHAM4 simulates a very large relative increase (more than 50%) compared to the other GCMs. If a larger suite of GCMs were available, the contribution by such outliers would be reduced.

[3]In NCAR DOE PCM, the edge of wintertime sea ice is apparently located south of Iceland in the control, north of Iceland in the future climate.

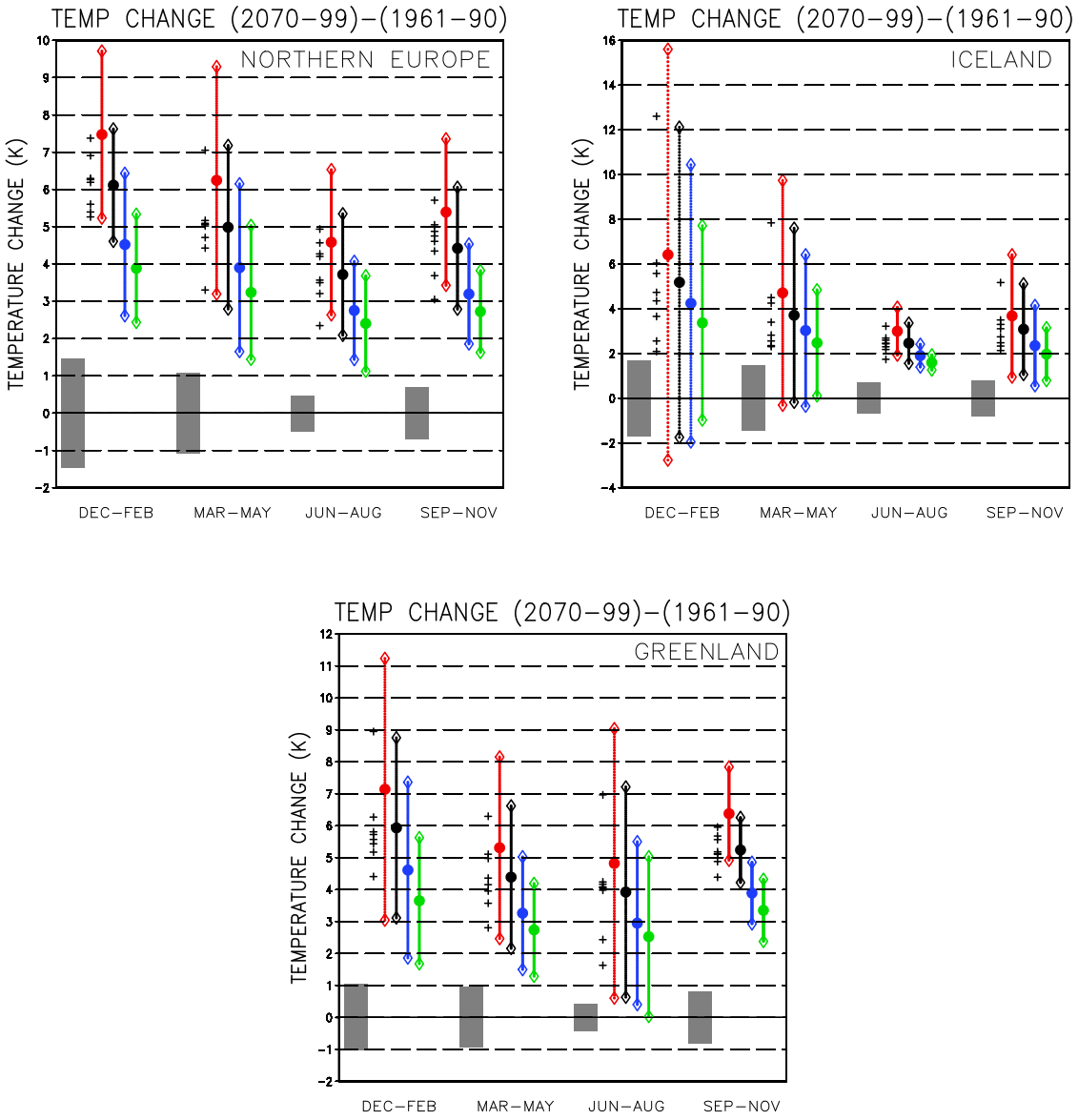

Fig. 3. GCM-based seasonal temperature change projections for Northern Europe (region "NEU", upper left panel), Iceland (region "ISL", upper right panel) and Greenland (region "GRÖ", lower panel). Thin coloured vertical bars represent the 95% probability interval of the temperature change from the period 1961–1990 to 2070–2099 as a response to the A1FI (red), A2 (black), B2 (blue) and B1 (green) forcing scenario. The dot at the centre of the bar denotes the medians of the intervals. Projections by individual GCM runs (only the A2 scenario depicted) are denoted by plus signs. Broad grey bars depict a measure of internal variability, i.e., ± 1.96 times the standard deviation of the differences between two arbitrarily-chosen 30-year averages, derived from standard deviation of temperature and precipitation in two millennial GCM runs with a constant atmospheric composition (see section 2.5).

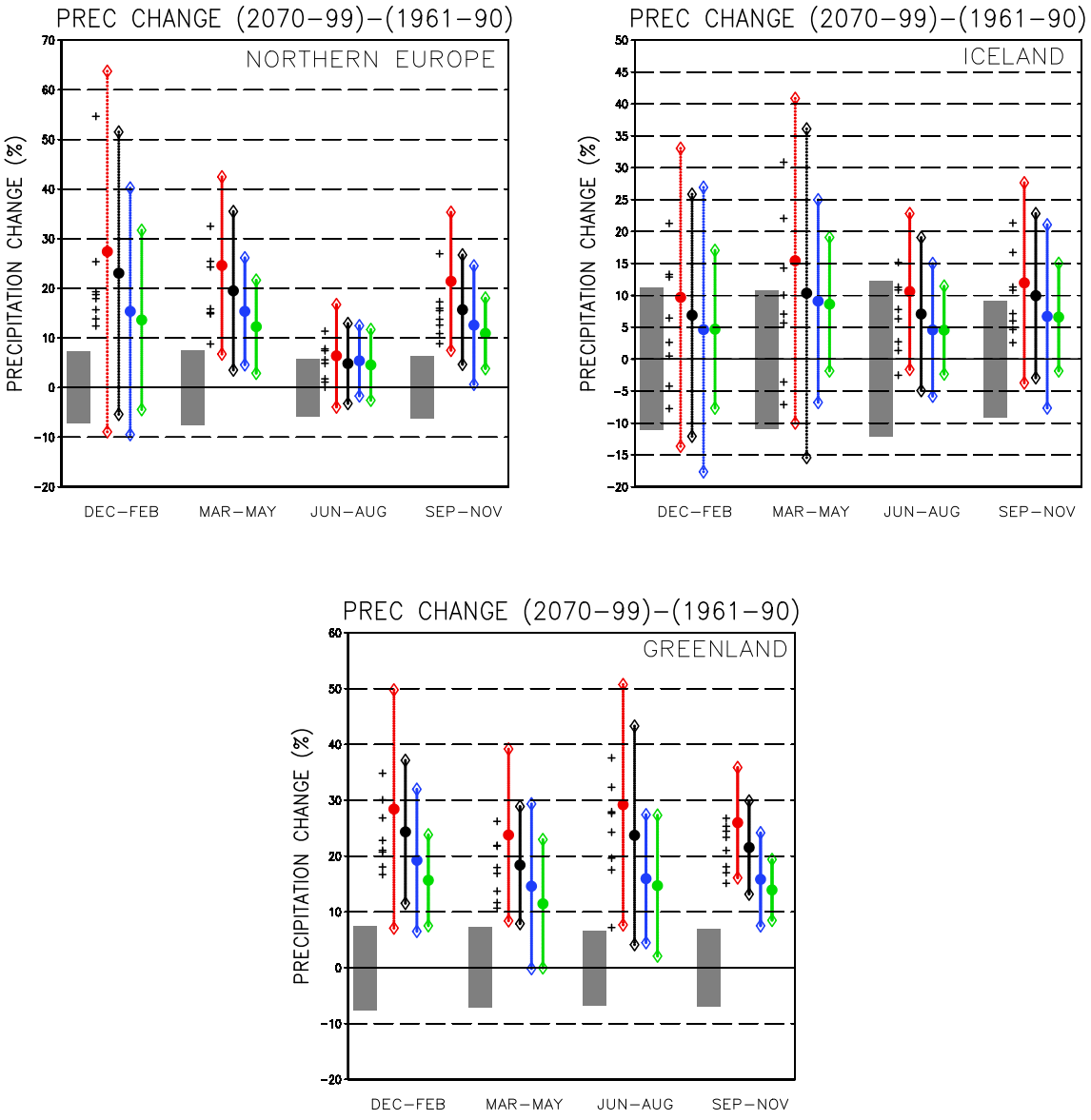

Fig. 4. GCM-based seasonal precipitation change projections for Northern Europe (region "NEU", upper left panel), Iceland (region "ISL", upper right panel) and Greenland (region "GRÖ", lower panel). For notations, see caption of Fig. 3.

The complete set of projections for the seven regions is tabulated in the Appendix. The tables include both the median estimates and the 95% probability intervals of temperature and precipitation change for the two projection periods. GCM-based projections are given for four SRES scenarios, RCM-based merely for the A2 scenario. A measure of internal variability is included to help assessing the signal-to-noise ratio of the projections.

Median temperature projections are statistically significant almost invariably. The only exceptions are the RCM-based projections for the Scandinavian region in winter and GCM-based projections for Iceland in spring, both of these solely for the first scenario period. Apart from Iceland (and winter of the 2021–2050 period for the "BAL" region under one scenario), both ends of the probability interval of temperature change are positive. Compared to the six-GCM projections, the PRUDENCE RCMs tend to project a weaker warming for winter and to some extent for spring. This holds both for the HadAM-forced RCMs and for the expanded set. In other seasons there is no systematic difference. For precipitation, the GCM and RCM projections are fairly consistent.

Median projections for precipitation change are not significant in several cases, especially so in summer. In Greenland by 2070–2099, however, precipitation is projected to increase significantly in all seasons. The 95% probability intervals typically intersect the zero line. Consequently, generally the sign of the future precipitation change cannot be established firmly.

Investigation of the projections shows that for the period 2021–2050 responses to the various forcing scenarios do not diverge markedly, whereas much larger differences are seen for the period 2070–2099.

4 Projected changes in climatic indices

In this section we discuss projected changes in a set of indices related to frost, snow cover and precipitation over the sub-domains SCA, FEN and BAL for the period 2071–2100. Unlike in the previous section, these projections are based on RCM experiments only. The acronyms for the individual RCM simulations use the conventions "RCM name – GCM – scenario". The code H refers to HadAM3H and E to ECHAM4/OPYC as the GCM providing the lateral boundary conditions.

The average annual numbers of frost days (FD) and days with snow cover (SCD) are projected to decrease by $\sim 20 - 40\%$ over the sub-regions "SCA" and "FEN", with a tendency to somewhat larger reduction over "BAL" (Fig. 5). The sign of the trends is consistent across all model simulations considered, irrespective of the forcing scenario and the driving GCM. Nonetheless, the ECHAM4/OPYC-driven RCM simulations produced larger changes in the indices

than the HadAM3H-driven ones, and the B2 radiative forcing resulted in smaller responses than the A2 forcing. In the BAL region, in particular, the projected annual mean decreases in FD were closely related to simulated increases in the DJF means of daily minimum temperature. Changes in SCD were clearly correlated with percentage decreases in the mean snow water equivalent, especially in the SCA and FEN regions (not shown). Reductions in the number of frost days lengthened the summer-time frost-free season: the date of the first autumnal (last vernal) frost was projected to occur two to five weeks later (earlier) than at present.

A trend towards heavier one-day precipitation amounts is rather robust in “SCA” and “FEN” in all seasons and in “BAL” during winter and spring (Fig. 6). The 30-year means of the winter and spring maximum one-day precipitation totals (designated as R1d) increase in every model experiment and sub-domain, the projected changes ranging up to 40% over “FEN” in

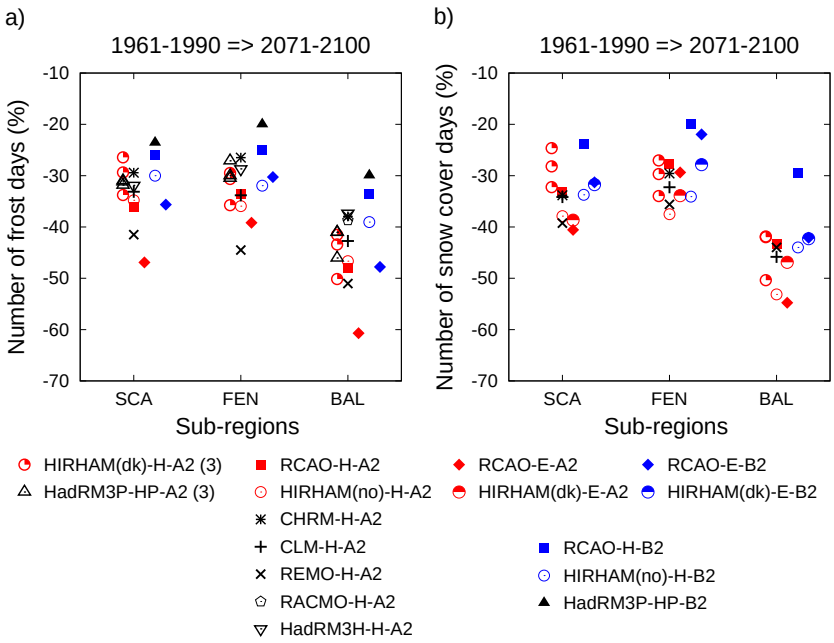

Fig. 5. Projected changes (%) in the annual mean number of (a) frost days and (b) snow cover days over regions “SCA”, “FEN” and “BAL” for the period 2071–2100, relative to the mean of 1961–1990. The symbols refer to the various RCM experiments (see legend). The acronym of each experiment includes the RCM name, the driving GCM (H for HadAM3H, HP for HadAM3P, E for ECHAM4/OPYC), the SRES scenario (A2 or B2) and the number (in parentheses) of ensemble simulations. For each region, the individual experiments are shown in five vertical columns from left to right as follows: 1 (2): RCM-H-A2 with (without) parallel ensemble members, 3: RCM-E-A2, 4: RCM-H-B2, 5: RCM-E-B2. The coloured symbols refer to experiments employed to construct the CE Production Scenarios. Note that the set of experiments was not exactly the same for (a) and (b). See Table 2 for information about the RCMs.

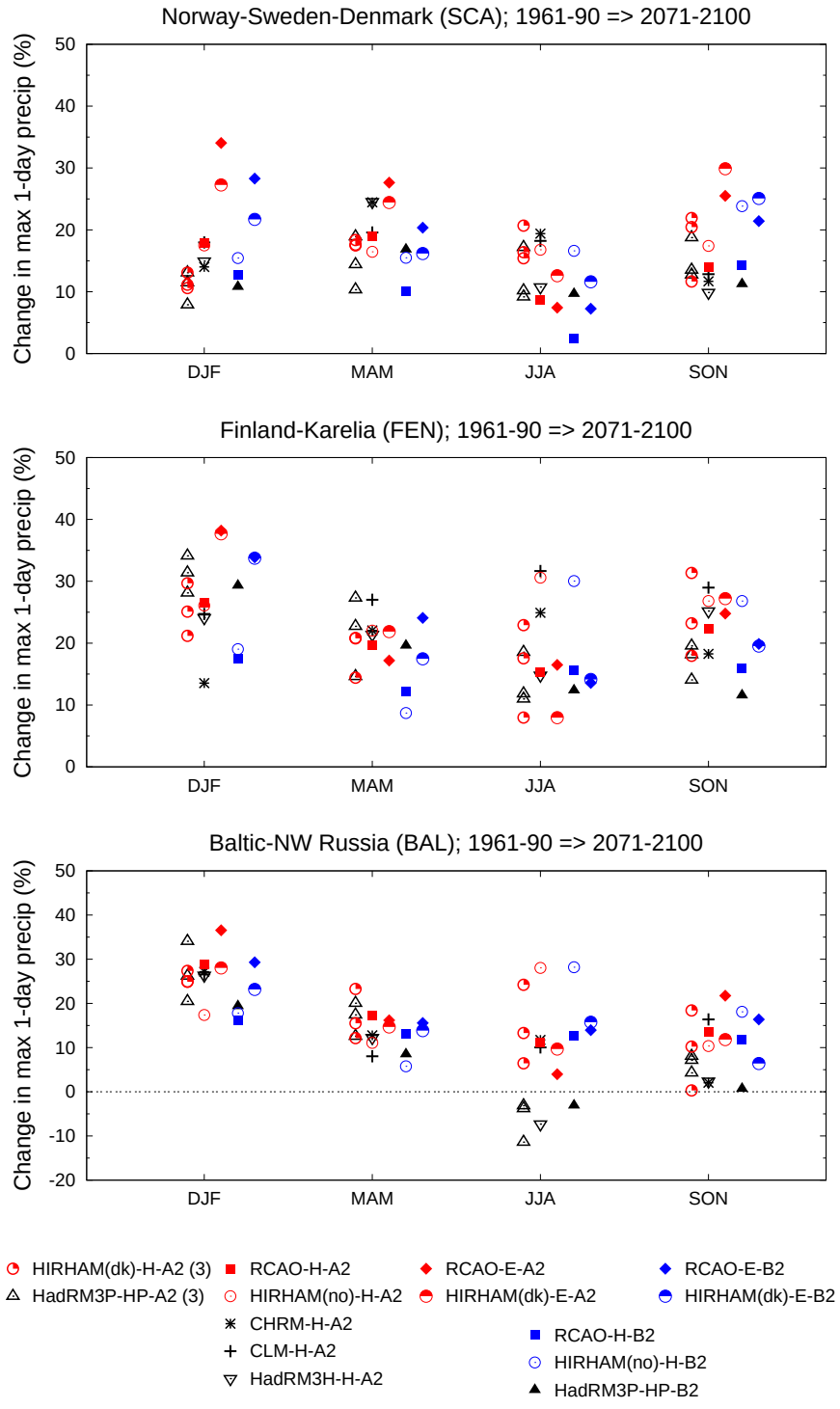

Fig. 6. RCM-simulated area-averaged changes (%) in the 30-year means of the greatest 1-day precipitation total in winter (DJF), spring (MAM), summer (JJA) and autumn (SON) for the period 2071–2100, relative to the baseline period 1961–1990, for regions "SCA", "FEN" and "BAL". For notations and details, see Fig. 5 and Table 2.

winter. In summer in “BAL”, however, the inter-model scatter is very large, and even the sign of the change is somewhat uncertain. The ECHAM4/OPYC-driven RCM simulations project larger changes in winter R1d than the HadAM3H-driven ones. This appears to be related to different responses in the wintertime atmospheric circulation in the two GCMs (RÄISÄNEN et al., 2004; CHRISTENSEN and CHRISTENSEN, 2006; DÉQUÉ et al., 2006). In other seasons the driving GCM had a less pronounced effect on the projected changes in R1d. When driven by the A2 forcing, the RCMs generally projected larger wintertime changes than they did under the B2 forcing. In summer (and in “FEN” and “BAL” in spring and autumn as well), the influence of random internal climate variability is so strong that the difference between the A2 and B2 responses is not clearly discernible.

The projected changes in R1d are closely correlated with simulated changes in mean precipitation (not shown). In winter the mean precipitation tends to increase more (in %) than the one-day extremes, the situation being vice versa in the other seasons. For “BAL” in summer, it was found that the models suggesting decreases in R1d (Fig. 6) produced even larger reductions in the mean precipitation, while several experiments with negligible changes in the mean nonetheless yielded increases in the one-day extreme. These findings are in agreement with BENISTON et al. (2006) and CARTER et al. (2005). On the other hand, future changes in droughts in the three sub-domains are highly uncertain as both decreases and increases were projected for the mean annual maximum length of dry periods by the various RCM simulations (not shown).

5 Summary and discussion

In the CE project, the production scenarios are based on RCM simulations with boundary data from two global models. Moreover, only two SRES scenarios have been examined. Consequently it is clear that these simulations cannot comprise the full uncertainty of future climate evolution.

In this report, climate projections for two tridecadal periods of the 21th century are constructed for seven discrete regions, covering Nordic and Baltic countries, north-western Russia and Greenland. Mean temperature and precipitation projections are based on six global coupled GCMs employed in the third assessment report of IPCC (2001). For comparison, projections derived from a set of RCMs participating in the PRUDENCE project are formulated as well. GCM projections are composed for four SRES scenarios: A1FI, A2, B2 and B1. For most of the models the A1FI and B1 projections are calculated applying a super-ensemble pattern-scaling method. RCM projections are only given for the A2 scenario, responses for the first

scenario period 2021–2050 being scaled in time from responses for the period 2071–2100. Examples of the regional projections are illustrated in section 3, while the full set is tabulated in the Appendix.

For several practical applications, changes in the frequency or amplitude of a certain meteorological phenomenon may be of larger interest than changes in the time-mean climate. Accordingly, section 4 of this report presents projections for climatological indices related to frost, snow and heavy precipitation. These indices are calculated for the Nordic mainland from the PRUDENCE RCM data.

The best estimates of temperature change, i.e., the six-GCM weighted mean responses, were found to be statistically significant almost invariably. Warming is generally stronger in winter than in summer. For the period 2070–2099, the A1FI forcing produces a warming nearly double that of B1. Still, the 95% probability intervals representing the various forcing scenarios overlap strongly.

Projected changes in the mean precipitation remain statistically insignificant in several cases, especially so in summer. The 95% probability intervals of temperature change typically intersect the zero line, i.e., the sign of the future precipitation change cannot be established firmly.

In winter and to some extent in spring, the RCMs employed for composing the CE production scenarios (RUMMUKAINEN, 2006) tend to simulate somewhat weaker warming than the present GCM median estimate, while their simulated precipitation increase is stronger. This especially holds for the A2 scenario. On the other hand, in summer the CE production scenarios for precipitation have a dry bias. In other cases systematic differences are fairly small, but there is a large scatter among the various CE RCM precipitation projections.

In accord with the general warming trend, the annual number of frost days tends to decrease by 20–50% from 1961–1990 to 2071–2100, some simulations giving even stronger reduction for the Baltic countries. The summer frost-free season is lengthened by 2–5 weeks at both ends. The number of snow cover days is reduced by 20–40% in Scandinavia and Fennoscandia, by 30–60% in Baltic countries. For both indices, ECHAM4-driven RCM experiments yield stronger responses than the HadAM3-driven ones.

In Fennoscandia, the seasonal maximum one-day precipitation increases by about 10–30%, in winter possibly even more. In summer, maximum precipitation tendencies are stronger than those in the mean precipitation. In the Baltic and Scandinavian regions, tendencies in the summertime maximum precipitation are weaker than those in Fennoscandia, but a tendency toward a more extreme summer precipitation climate is apparent anyhow.

Acknowledgements

This work has been financed by Nordic Energy Research (NEFP). The time series of the GCM-simulated temperatures and precipitation amounts were downloaded from the Intergovernmental Panel for Climate Change Data Distribution Centre (http://ipcc-ddc.cru.uea.ac.uk/dkrz/dkrz_index.html), whilst some of the HadCM3 runs have been provided by Dr. D. Viner. The millennial CGCM2 control run data were provided by Drs. Francis Zwiers and Slava Kharin. The PRUDENCE RCM data were downloaded from http://prudence.dmi.dk.

References

BENISTON, M, STEPHENSON, D.B., CHRISTENSEN, O.B., FERRO, C.A.T., FREI, C., GOYETTE, S., HALSNAES, K. HOLT, T. JYLHÄ, K. KOFFI, B. PALUTIKOF, J., SCHÖLL, R., SEMMLER T. and WOTH, K., 2006. Future Extreme Events in European Climate: An Exploration of Regional Climate Model Projections. *Climatic Change*, PRUDENCE special issue.

CARTER, T.R., JYLHÄ, K., PERRELS, A., FRONZEK, S. and KANKAANPÄÄ, S., 2005. FINADAPT scenarios for the 21st century: alternative futures for considering adaptation to climate change in Finland. FINADAPT working paper 2. *Finnish Environment Institute Mimeographs* 332, 42 p.

CHRISTENSEN, J.H., CARTER, T.R. and RUMMUKAINEN, M., 2006. Evaluating the performance and utility of regional climate models: the PRUDENCE project. *Clim. Change*, PRUDENCE special issue.

CHRISTENSEN, J.H. and CHRISTENSEN, O.B., 2006. A summary of the PRUDENCE model projections of changes in European climate during this century. *Clim. Change*, PRUDENCE special issue.

CHRISTENSEN, J.H., RÄISÄNEN, J., IVERSEN, T., BJØRGE, D., CHRISTENSEN, O.B. and RUMMUKAINEN, M., 2001. A synthesis of regional climate change simulations – A Scandinavian perspective. *Geophys. Res. Lett.*, **28**, 1003-1006.

DÉQUÉ, M., ROWELL, D.P., LÜTHI, D., GIORGI, F., CHRISTENSEN, J.H., ROCKEL, B., JACOB, D., KJELLSTRÖM, E., DE CASTRO, M. and VAN DEN HURK, B., 2006. An intercomparison of regional climate simulations for Europe: assessing uncertainties in model projections. *Clim. Change*, PRUDENCE special issue.

ENGEN-SKAUGEN, T., ROALD, L.A., BELDRING, S., FØRLAND, E.J., TVEITO, O.E., ENGELAND, K. and BENESTAD, R., 2005. Climate change impacts on water balance in Norway. *Met.no report* **1/2005**, Norwegian Meteorological Institute, 82 p.

IPCC, 2001. *Climate Change 2001: The Scientific Basis. Contribution of Working Group I to the Third Assessment Report of the Intergovernmental Panel on Climate Change* [HOUGHTON, J.T., DING, Y., GRIGGS, D.J., NOGUER, M., VAN DER LINDEN, P.J., DAI, X., MASKELL, K. and JOHNSON, C.A. (eds.)]. Cambridge University Press, Cambridge and New York, 881 pp.

JYLHÄ, K., FRONZEK, S., TUOMENVIRTA, H., CARTER, T.R. and RUOSTEENOJA, K., 2006. Changes in frost, snow and Baltic sea ice by the end of the 21st century based on climate model projections for Europe. Submitted to *Clim. Change*.

MCAVANEY, B.J., COVEY, C., JOUSSAUME, S. KATTSOV, V., KITOH, A., OGANA, W., PITMAN, A.J., WEAVER, A.J., WOOD, R.A. and ZHAO, Z.-C., 2001. Model evaluation. In: *Climate Change 2001: The Scientific Basis. Contribution of Working Group I to the Third Assessment Report of the Intergovernmental Panel on Climate Change* [HOUGHTON, J.T., DING, Y., GRIGGS, D.J., NOGUER, M., VAN DER LINDEN, P.J., DAI, X., MASKELL, K. and JOHNSON, C.A. (eds.)]. Cambridge University Press, Cambridge and New York, pp. 471-523.

RAPER, S.C.B, GREGORY, J.M. and OSBORN, T.J., 2001. Use of a upwhelling-diffusion energy balance climate model to simulate and diagnose A/OGCM results. *Clim. Dyn.*, **17**, 601-613.

RUMMUKAINEN, M., 2006. The CE regional climate scenarios. European conference of impacts of climate change on renewable energy sources. Reykjavik, Iceland, 5-9 June 2006.

RUOSTEENOJA, K., TUOMENVIRTA, H. and JYLHÄ, K., 2006. GCM-based regional temperature and precipitation change estimates for Europe under four SRES scenarios applying a super-ensemble pattern-scaling method. *Clim. Change*, PRUDENCE special issue.

RÄISÄNEN, J., HANSSON, U., ULLERSTIG, A., DÖSCHER, R., GRAHAM, L.P., JONES, C., MEIER, H.E.M., SAMUELSSON, P. and WILLÉN, U., 2004. European climate in the late twenty-first century: regional simulations with two driving global models and two forcing scenarios. *Clim. Dyn.*, **22**, 13-31.

Appendix: Regional projections tabulated

Temperature projections for the seven regions defined in section 1 are listed in Table A1, precipitation responses in Table A2. GCM-based projections (columns 2–5) are given separately for four SRES forcing scenarios (A1FI, A2, B2, B1). Columns 6–7 include the RCM-based projections, derived from the suite of HadCM3-forced PRUDENCE RCM simulations (RCMHAD) and from the extended set including (real or surrogate) simulations with three boundary models (RCMEXT; see section 2.4). PRUDENCE RCMs do not cover Iceland and Greenland. For all projections, the median estimate is given, with the 95% probability interval parenthesized. Projections that are based entirely or partly on approximative pattern-scaled responses are italicized: RCM projections for the period 2021–2050 are scaled in time (section 2.3), while GCM responses to the A1FI and B1 scenarios for most of the GCMs are scaled applying the super-ensemble method (section 2.2). Projections are given separately for two time spans (2021–2050 and 2070–2099, the baseline period being 1961–1990) and four seasons. The last column includes the 97.5% quantile for the difference between two independent tridecadal means, derived from internal variability in millennial GCM runs (section 2.5). Projections with the absolute value exceeding that measure of internal value are statistically significant at the 5% level and are denoted by an asterix.

Table A1. Seasonal temperature responses for the regions shown in Fig. 1. Unit °C.

REGION NEU

	GCM-A1FI	GCM-A2	GCM-B2	GCM-B1	RCMHAD-A2	RCMEXT-A2	INT.VAR
DEC-FEB							
2021–2050	** 3.0(1.3 – 4.6)*	* 2.6(0.8 – 4.4)	* 2.6(1.2 – 4.0)	** 2.4(1.0 – 3.7)*	** 1.5(1.3 – 1.8)*	** 1.7(1.1 – 2.3)*	1.5
2070–2099	** 7.5(5.2 – 9.7)*	* 6.1(4.6 – 7.6)	* 4.5(2.6 – 6.4)	** 3.9(2.4 – 5.3)*	* 4.5(3.8 – 5.2)	* 5.0(3.2 – 6.7)	
MAR-MAY							
2021–2050	** 2.4(0.6 – 4.1)*	* 2.2(0.7 – 3.6)	* 2.1(0.1 – 4.0)	** 1.9(0.5 – 3.4)*	** 1.3(1.1 – 1.6)*	** 1.4(0.9 – 1.9)*	1.1
2070–2099	** 6.2(3.2 – 9.3)*	* 5.0(2.8 – 7.2)	* 3.9(1.7 – 6.2)	** 3.2(1.4 – 5.0)*	* 3.9(3.2 – 4.6)	* 4.1(2.7 – 5.5)	
JUN-AUG							
2021–2050	** 1.8(1.1 – 2.6)*	* 1.6(0.9 – 2.3)	* 1.6(1.0 – 2.2)	** 1.4(0.9 – 1.9)*	** 1.1(0.7 – 1.6)*	** 1.2(0.7 – 1.7)*	0.5
2070–2099	** 4.6(2.6 – 6.5)*	* 3.7(2.1 – 5.3)	* 2.8(1.4 – 4.1)	** 2.4(1.1 – 3.7)*	* 3.3(2.1 – 4.5)	* 3.5(2.1 – 4.9)	
SEP-NOV							
2021–2050	** 2.0(1.1 – 2.9)*	* 1.9(0.9 – 2.9)	* 1.7(0.7 – 2.7)	** 1.6(0.9 – 2.4)*	** 1.5(1.2 – 1.9)*	** 1.5(1.1 – 1.9)*	0.7
2070–2099	** 5.4(3.4 – 7.4)*	* 4.4(2.8 – 6.1)	* 3.2(1.9 – 4.5)	** 2.7(1.6 – 3.8)*	* 4.4(3.4 – 5.4)	* 4.5(3.2 – 5.7)	

REGION SCA

	GCM-A1FI	GCM-A2	GCM-B2	GCM-B1	RCMHAD-A2	RCMEXT-A2	INT.VAR
DEC-FEB							
2021–2050	** 2.5(1.7 – 3.3)*	* 2.2(1.3 – 3.2)	* 2.2(1.3 – 3.1)	** 2.0(1.3 – 2.7)*	*1.3(1.1 – 1.5)*	*1.4(0.8 – 2.0)*	1.5
2070–2099	** 6.4(5.2 – 7.5)*	* 5.3(4.4 – 6.2)	* 3.8(2.7 – 5.0)	** 3.3(2.5 – 4.1)*	* 3.7(3.1 – 4.2)	* 4.1(2.3 – 5.9)	
MAR-MAY							
2021–2050	** 2.2(0.6 – 3.7)*	* 2.0(0.6 – 3.3)	* 1.8(0.1 – 3.6)	** 1.7(0.4 – 3.1)*	** 1.2(0.9 – 1.5)*	** 1.3(0.8 – 1.8)*	1.2
2070–2099	** 5.7(3.2 – 8.1)*	* 4.6(2.8 – 6.3)	* 3.5(1.6 – 5.4)	** 3.0(1.5 – 4.4)*	* 3.5(2.7 – 4.2)	* 3.8(2.2 – 5.4)	
JUN-AUG							
2021–2050	** 1.7(1.1 – 2.2)*	* 1.5(0.9 – 2.1)	* 1.5(1.0 – 1.9)	** 1.3(0.8 – 1.7)*	** 1.1(0.8 – 1.4)*	** 1.1(0.7 – 1.6)*	0.5
2070–2099	** 4.3(2.9 – 5.6)*	* 3.5(2.3 – 4.7)	* 2.6(1.7 – 3.6)	** 2.2(1.3 – 3.1)*	* 3.2(2.2 – 4.1)	* 3.4(2.1 – 4.6)	
SEP-NOV							
2021–2050	** 1.8(1.2 – 2.5)*	* 1.7(0.8 – 2.7)	* 1.6(0.9 – 2.2)	** 1.5(0.9 – 2.0)*	** 1.4(1.1 – 1.8)*	** 1.4(1.0 – 1.8)*	0.7
2070–2099	** 4.9(3.6 – 6.2)*	* 4.0(2.8 – 5.2)	* 2.9(2.0 – 3.8)	** 2.5(1.7 – 3.3)*	* 4.2(3.1 – 5.2)	* 4.2(3.1 – 5.4)	

REGION FEN

	GCM-A1FI	GCM-A2	GCM-B2	GCM-B1	RCMHAD-A2	RCMEXT-A2	INT.VAR
DEC-FEB							
2021–2050	** 3.5(1.3 – 5.6)*	* 3.0(0.6 – 5.5)	* 3.0(1.3 – 4.7)	** 2.8(1.1 – 4.5)*	** 1.8(1.5 – 2.1)*	** 2.0(1.3 – 2.6)*	1.7
2070–2099	** 8.8(5.5 – 12.0)*	* 7.1(4.8 – 9.4)	* 5.4(2.7 – 8.1)	** 4.6(2.5 – 6.7)*	* 5.2(4.3 – 6.2)	* 5.7(3.9 – 7.6)	
MAR-MAY							
2021–2050	** 2.6(0.6 – 4.6)*	* 2.4(0.9 – 4.0)	* 2.2(0.0 – 4.5)	** 2.2(0.4 – 3.9)*	** 1.5(1.1 – 1.9)*	** 1.5(1.1 – 2.0)*	1.2
2070–2099	** 7.0(3.4 – 10.6)*	* 5.5(3.0 – 8.1)	* 4.4(1.8 – 7.0)	** 3.7(1.4 – 5.9)*	* 4.4(3.2 – 5.5)	* 4.5(3.1 – 5.9)	
JUN-AUG							
2021–2050	** 1.9(1.2 – 2.7)*	* 1.7(0.9 – 2.4)	* 1.7(1.1 – 2.3)	** 1.5(1.0 – 2.0)*	** 1.1(0.7 – 1.5)*	** 1.2(0.8 – 1.6)*	0.5
2070–2099	** 4.7(2.6 – 6.9)*	* 3.8(2.0 – 5.6)	* 2.8(1.4 – 4.3)	** 2.5(1.0 – 4.0)*	* 3.3(2.2 – 4.4)	* 3.4(2.2 – 4.6)	
SEP-NOV							
2021–2050	** 2.3(1.1 – 3.5)*	* 2.1(0.8 – 3.3)	* 1.9(0.6 – 3.2)	** 1.9(0.9 – 2.9)*	** 1.6(1.2 – 2.0)*	** 1.6(1.2 – 2.0)*	0.8
2070–2099	** 5.9(3.4 – 8.3)*	* 4.8(2.8 – 6.9)	* 3.5(1.8 – 5.2)	** 2.9(1.6 – 4.3)*	* 4.6(3.5 – 5.8)	* 4.8(3.5 – 6.0)	

REGION BAL

	GCM-A1FI	GCM-A2	GCM-B2	GCM-B1	RCMHAD-A2	RCMEXT-A2	INT.VAR
DEC-FEB							
2021–2050	** 3.1(0.1 – 6.0)*	* 2.7(-0.2 – 5.6)	* 2.7(0.1 – 5.2)	** 2.5(0.1 – 4.8)*	** 1.7(1.4 – 2.1)*	** 1.8(1.2 – 2.4)*	1.5
2070–2099	** 7.5(3.6 – 11.5)*	* 6.2(3.4 – 8.9)	* 4.5(1.5 – 7.5)	** 3.9(1.7 – 6.0)*	* 5.1(4.2 – 6.0)	* 5.4(3.6 – 7.1)	
MAR-MAY							
2021–2050	** 2.4(0.4 – 4.4)*	* 2.2(0.5 – 3.8)	* 2.2(0.0 – 4.4)	** 2.0(0.4 – 3.6)*	** 1.4(1.2 – 1.6)*	** 1.4(0.8 – 1.9)*	1.2
2070–2099	** 6.1(2.5 – 9.8)*	* 4.9(2.2 – 7.7)	* 3.8(1.2 – 6.5)	** 3.1(1.2 – 5.0)*	* 4.1(3.4 – 4.8)	* 4.1(2.5 – 5.7)	
JUN-AUG							
2021–2050	** 2.1(0.8 – 3.3)*	* 1.8(0.6 – 2.9)	* 1.8(0.7 – 3.0)	** 1.6(0.8 – 2.5)*	** 1.3(0.6 – 1.9)*	** 1.3(0.5 – 2.1)*	0.6
2070–2099	** 4.9(2.1 – 7.8)*	* 4.0(1.7 – 6.3)	* 2.9(1.0 – 4.8)	** 2.6(0.9 – 4.3)*	* 3.7(1.7 – 5.7)	* 3.8(1.5 – 6.1)	
SEP-NOV							
2021–2050	** 2.0(0.9 – 3.1)*	* 1.8(0.8 – 2.9)	* 1.8(0.5 – 3.1)	** 1.7(0.8 – 2.5)*	** 1.5(1.2 – 1.9)*	** 1.5(1.0 – 2.1)*	0.7
2070–2099	** 5.6(3.0 – 8.3)*	* 4.6(2.5 – 6.7)	* 3.3(1.6 – 5.1)	** 2.9(1.4 – 4.3)*	* 4.4(3.4 – 5.4)	* 4.5(2.9 – 6.1)	

REGION ÖST

	GCM-A1FI	GCM-A2	GCM-B2	GCM-B1	RCMHAD-A2	RCMEXT-A2	INT.VAR
DEC-FEB							
2021–2050	** 2.6(1.1 – 4.1)*	* 2.3(0.8 – 3.9)	* 2.3(0.9 – 3.7)	** 2.1(0.9 – 3.3)*	** 1.3(1.1 – 1.5)*	** 1.4(0.8 – 2.0)*	1.2
2070–2099	** 6.4(4.3 – 8.6)*	* 5.3(3.8 – 6.8)	* 3.8(2.0 – 5.6)	** 3.3(2.3 – 4.3)*	* 3.8(3.1 – 4.4)	* 4.0(2.3 – 5.8)	
MAR-MAY							
2021–2050	** 2.2(0.3 – 4.0)*	* 1.9(0.4 – 3.5)	* 1.9(0.0 – 3.8)	** 1.8(0.3 – 3.2)*	** 1.2(1.0 – 1.4)*	** 1.2(0.6 – 1.9)*	1.0
2070–2099	** 5.5(2.6 – 8.4)*	* 4.4(2.3 – 6.6)	* 3.4(1.3 – 5.4)	** 2.8(1.3 – 4.4)*	* 3.5(2.9 – 4.1)	* 3.7(1.9 – 5.5)	
JUN-AUG							
2021–2050	** 2.1(0.8 – 3.5)*	* 1.8(0.8 – 2.9)	* 1.9(0.8 – 2.9)	** 1.7(0.7 – 2.7)*	** 1.8(1.4 – 2.1)*	** 1.4(0.5 – 2.2)*	0.7
2070–2099	** 5.2(2.0 – 8.5)*	* 4.3(1.6 – 6.9)	* 3.2(1.0 – 5.4)	** 2.8(0.7 – 4.9)*	* 5.1(4.2 – 6.0)	* 4.0(1.6 – 6.4)	
SEP-NOV							
2021–2050	** 2.1(1.3 – 2.9)*	* 1.9(1.2 – 2.6)	* 1.8(1.0 – 2.6)	** 1.7(1.1 – 2.3)*	** 1.7(1.4 – 1.9)*	** 1.5(0.9 – 2.0)*	0.7
2070–2099	** 5.4(3.1 – 7.7)*	* 4.4(2.6 – 6.2)	* 3.2(1.7 – 4.8)	** 2.8(1.5 – 4.2)*	* 4.9(4.1 – 5.6)	* 4.3(2.7 – 6.0)	

REGION ISL

	GCM-A1FI	GCM-A2	GCM-B2	GCM-B1	RCMHAD-A2	RCMEXT-A2	INT.VAR
DEC-FEB							
2021–2050	** 2.4(-1.6 – 6.4)*	* 2.1(-1.2 – 5.5)	* 2.2(-2.0 – 6.3)	** 1.9(-1.3 – 5.2)*	—	—	1.7
2070–2099	** 6.4(-2.8 – 15.6)*	* 5.2(-1.7 – 12.1)	* 4.2(-2.0 – 10.4)	** 3.4(-1.0 – 7.7)*	—	—	
MAR-MAY							
2021–2050	** 1.7(-0.4 – 3.8)*	1.4(-0.6 – 3.4)	* 1.5(-0.4 – 3.5)	*1.2(-0.6 – 3.1)*	—	—	1.5
2070–2099	** 4.7(-0.3 – 9.7)*	* 3.7(-0.2 – 7.6)	* 3.0(-0.4 – 6.4)	** 2.5(0.1 – 4.8)*	—	—	
JUN-AUG							
2021–2050	** 1.1(0.7 – 1.6)*	* 1.0(0.6 – 1.4)	* 1.0(0.6 – 1.5)	** 0.8(0.2 – 1.5)*	—	—	0.7
2070–2099	** 3.0(1.9 – 4.1)*	* 2.5(1.6 – 3.4)	* 1.9(1.4 – 2.4)	** 1.6(1.3 – 1.9)*	—	—	
SEP-NOV							
2021–2050	** 1.5(-0.2 – 3.2)*	* 1.4(-0.1 – 2.9)	* 1.4(-0.1 – 2.9)	** 1.1(-0.5 – 2.7)*	—	—	0.8
2070–2099	** 3.7(1.0 – 6.4)*	* 3.1(1.1 – 5.1)	* 2.4(0.6 – 4.1)	** 2.0(0.8 – 3.2)*	—	—	

REGION GRÖ

	GCM-A1FI	GCM-A2	GCM-B2	GCM-B1	RCMHAD-A2	RCMEXT-A2	INT.VAR
DEC-FEB							
2021–2050	** 2.6(0.4 – 4.9)*	* 2.5(0.4 – 4.6)	* 2.5(0.5 – 4.4)	** 2.1(0.1 – 4.1)*	—	—	1.0
2070–2099	** 7.1(3.0 – 11.2)*	* 5.9(3.1 – 8.8)	* 4.6(1.9 – 7.4)	** 3.7(1.7 – 5.6)*	—	—	
MAR-MAY							
2021–2050	** 1.9(0.5 – 3.4)*	* 1.7(0.3 – 3.1)	* 1.8(0.6 – 3.1)	** 1.5(0.1 – 2.9)*	—	—	1.0
2070–2099	** 5.3(2.5 – 8.2)*	* 4.4(2.2 – 6.6)	* 3.3(1.5 – 5.0)	** 2.7(1.3 – 4.2)*	—	—	
JUN-AUG							
2021–2050	** 1.9(0.3 – 3.5)*	* 1.8(0.3 – 3.2)	* 1.7(0.2 – 3.2)	** 1.6(0.2 – 3.0)*	—	—	0.4
2070–2099	** 4.8(0.6 – 9.0)*	* 3.9(0.6 – 7.2)	* 3.0(0.4 – 5.5)	** 2.5(0.0 – 5.0)*	—	—	
SEP-NOV							
2021–2050	** 2.5(2.0 – 3.0)*	* 2.2(1.6 – 2.8)	* 2.2(1.8 – 2.7)	** 1.9(1.2 – 2.7)*	—	—	0.8
2070–2099	** 6.4(4.9 – 7.8)*	* 5.2(4.2 – 6.3)	* 3.9(2.9 – 4.9)	** 3.4(2.4 – 4.3)*	—	—	

Table A2. Seasonal precipitation responses for the regions shown in Fig. 1. Unit %.

REGION NEU

	GCM-A1FI	GCM-A2	GCM-B2	GCM-B1	RCMHAD-A2	RCMEXT-A2	INT.VAR
DEC-FEB							
2021–2050	** 11(-10 – 32)*	* 11(-8 – 30)	* 9(-11 – 29)	** 9(-9 – 26)*	** 8(5 – 10)*	** 9(0 – 17)*	7.2
2070–2099	** 27(-9 – 64)*	* 23(-5 – 52)	* 15(-9 – 40)	** 14(-4 – 32)*	* 22(14 – 30)	* 25(0 – 50)	
MAR-MAY							
2021–2050	** 9(-4 – 21)*	* 8(-5 – 20)	* 10(1 – 19)	** 8(-1 – 17)*	*5(1 – 8)*	*5(-3 – 14)*	7.5
2070–2099	** 25(7 – 42)*	* 20(4 – 35)	* 15(5 – 26)	** 12(3 – 22)*	* 14(4 – 23)	* 16(-9 – 41)	
JUN-AUG							
2021–2050	*5(0 – 10)*	4(0 – 8)	6(0 – 11)	*4(0 – 7)*	*1(-3 – 6)*	*1(-4 – 6)*	5.8
2070–2099	** 6(-4 – 17)*	5(-3 – 13)	5(-2 – 12)	*5(-3 – 12)*	4(-10 – 18)	2(-12 – 16)	
SEP-NOV							
2021–2050	** 6(-1 – 13)*	6(0 – 12)	6(-3 – 15)	*5(0 – 11)*	*3(-1 – 7)*	*5(-3 – 13)*	6.3
2070–2099	** 21(7 – 35)*	* 16(5 – 27)	* 13(1 – 25)	** 11(4 – 18)*	* 8(-3 – 19)	* 15(-9 – 39)	

REGION SCA

	GCM-A1FI	GCM-A2	GCM-B2	GCM-B1	RCMHAD-A2	RCMEXT-A2	INT.VAR
DEC-FEB							
2021–2050	** 10(-10 – 29)*	* 9(-9 – 27)	7(-12 – 26)	*7(-9 – 23)*	*6(2 – 9)*	*7(-2 – 16)*	8.1
2070–2099	** 24(-7 – 54)*	* 20(-4 – 44)	* 12(-11 – 35)	** 12(-4 – 27)*	* 17(6 – 27)	* 21(-5 – 47)	
MAR-MAY							
2021–2050	** 9(-2 – 19)*	* 8(-4 – 20)	* 8(0 – 16)	*8(0 – 15)*	*5(2 – 7)*	*6(-3 – 15)*	8.1
2070–2099	** 23(3 – 42)*	* 19(1 – 37)	* 14(4 – 24)	** 12(2 – 21)*	* 14(7 – 22)	* 18(-8 – 43)	
JUN-AUG							
2021–2050	** 7(-1 – 15)*	4(-1 – 9)	6(0 – 13)	*5(0 – 9)*	*0(-4 – 4)*	*1(-3 – 4)*	6.8
2070–2099	** 9(-3 – 21)*	* 7(-4 – 18)	6(-1 – 14)	*6(-3 – 14)*	0(-11 – 12)	2(-10 – 13)	
SEP-NOV							
2021–2050	*6(-1 – 14)*	6(0 – 13)	6(-3 – 15)	*5(-2 – 12)*	*3(0 – 7)*	*5(-3 – 13)*	7.5
2070–2099	** 22(9 – 35)*	* 16(6 – 27)	* 12(1 – 24)	** 10(3 – 17)*	* 10(-1 – 20)	* 16(-8 – 40)	

REGION FEN

	GCM-A1FI	GCM-A2	GCM-B2	GCM-B1	RCMHAD-A2	RCMEXT-A2	INT.VAR
DEC-FEB							
2021–2050	** 13(-10 – 37)*	* 13(-11 – 36)	* 11(-10 – 31)	** 10(-9 – 30)*	** 10(7 – 13)*	** 11(1 – 20)*	8.1
2070–2099	** 32(-11 – 76)*	* 27(-8 – 61)	* 19(-9 – 47)	** 16(-5 – 38)*	* 28(19 – 37)	* 31(3 – 60)	
MAR-MAY							
2021–2050	** 9(-7 – 26)*	8(-7 – 24)	* 11(-3 – 25)	*9(-3 – 22)*	*5(1 – 9)*	*5(-4 – 15)*	9.2
2070–2099	** 27(5 – 50)*	* 21(2 – 41)	* 17(3 – 32)	** 14(2 – 27)*	* 14(2 – 26)	* 16(-13 – 44)	
JUN-AUG							
2021–2050	*7(-1 – 16)*	6(-1 – 12)	8(-5 – 21)	*5(-2 – 11)*	*4(-2 – 10)*	*3(-4 – 9)*	8.5
2070–2099	** 9(-5 – 23)*	6(-6 – 19)	7(-3 – 17)	*7(-5 – 19)*	* 12(-6 – 31)	8(-11 – 27)	
SEP-NOV							
2021–2050	*8(-1 – 16)*	7(-1 – 15)	6(-4 – 16)	*6(0 – 13)*	*4(0 – 8)*	*7(-2 – 15)*	7.6
2070–2099	** 23(4 – 43)*	* 17(2 – 32)	* 15(-2 – 31)	** 12(2 – 21)*	* 12(1 – 23)	* 20(-6 – 45)	

REGION BAL

	GCM-A1FI	GCM-A2	GCM-B2	GCM-B1	RCMHAD-A2	RCMEXT-A2	INT.VAR
DEC-FEB							
2021–2050	* 13(-10 – 35)	* 12(-6 – 30)	* 11(-12 – 35)	* 10(-8 – 28)	* 10(6 – 14)	* 10(3 – 18)	9.3
2070–2099	* 31(-12 – 74)	* 26(-8 – 60)	* 18(-9 – 45)	* 16(-5 – 37)	* 29(18 – 40)	* 31(8 – 53)	
MAR-MAY							
2021–2050	8(-7 – 22)	5(-10 – 21)	* 11(5 – 17)	8(-1 – 16)	4(-4 – 13)	4(-6 – 15)	9.9
2070–2099	* 24(10 – 39)	* 18(5 – 31)	* 16(2 – 29)	* 11(1 – 20)	* 13(-12 – 38)	* 13(-17 – 43)	
JUN-AUG							
2021–2050	0(-6 – 5)	1(-7 – 9)	0(-10 – 10)	0(-5 – 4)	1(-10 – 11)	-2(-13 – 9)	10.2
2070–2099	-2(-29 – 24)	-2(-21 – 18)	1(-16 – 18)	-1(-13 – 12)	2(-28 – 32)	-6(-39 – 26)	
SEP-NOV							
2021–2050	5(-3 – 13)	4(-3 – 10)	5(-7 – 16)	5(-2 – 12)	-1(-7 – 5)	2(-7 – 11)	8.7
2070–2099	* 17(3 – 31)	* 13(-2 – 27)	* 10(-3 – 23)	* 11(2 – 21)	-3(-20 – 14)	6(-21 – 32)	

REGION ÖST

	GCM-A1FI	GCM-A2	GCM-B2	GCM-B1	RCMHAD-A2	RCMEXT-A2	INT.VAR
DEC-FEB							
2021–2050	* 9(-8 – 27)	9(-5 – 22)	8(-10 – 26)	7(-7 – 22)	* 11(6 – 16)	* 9(1 – 17)	8.9
2070–2099	* 24(-6 – 55)	* 20(-4 – 44)	* 14(-8 – 37)	* 12(-4 – 27)	* 32(19 – 46)	* 27(4 – 50)	
MAR-MAY							
2021–2050	6(-10 – 22)	4(-11 – 20)	9(-3 – 21)	6(-7 – 19)	4(0 – 9)	4(-3 – 10)	9.2
2070–2099	* 18(1 – 35)	* 14(-1 – 28)	* 12(1 – 24)	8(-2 – 18)	* 13(0 – 26)	* 11(-8 – 30)	
JUN-AUG							
2021–2050	3(-4 – 9)	3(-3 – 9)	2(-7 – 11)	2(-4 – 9)	* 24(2 – 47)	* 10(-20 – 41)	8.6
2070–2099	-2(-22 – 18)	-2(-19 – 15)	1(-12 – 13)	0(-11 – 11)	* 71(5 –138)	* 30(-60 –120)	
SEP-NOV							
2021–2050	7(0 – 14)	6(0 – 11)	7(-2 – 15)	6(0 – 12)	* 12(2 – 22)	8(-10 – 25)	8.1
2070–2099	* 21(8 – 33)	* 15(3 – 26)	* 12(1 – 24)	* 12(3 – 20)	* 35(5 – 65)	* 23(-28 – 75)	

REGION ISL

	GCM-A1FI	GCM-A2	GCM-B2	GCM-B1	RCMHAD-A2	RCMEXT-A2	INT.VAR
DEC-FEB							
2021–2050	3(-8 – 13)	2(-9 – 13)	2(-13 – 18)	3(-6 – 11)	—	—	11.1
2070–2099	10(-14 – 33)	7(-12 – 26)	5(-18 – 27)	5(-8 – 17)	—	—	
MAR-MAY							
2021–2050	6(-11 – 22)	3(-10 – 17)	3(-9 – 14)	4(-8 – 15)	—	—	10.8
2070–2099	* 15(-10 – 41)	10(-15 – 36)	9(-7 – 25)	9(-2 – 19)	—	—	
JUN-AUG							
2021–2050	1(-7 – 9)	0(-11 – 11)	0(-11 – 12)	-1(-11 – 9)	—	—	12.2
2070–2099	11(-2 – 23)	7(-5 – 19)	5(-6 – 15)	5(-2 – 11)	—	—	
SEP-NOV							
2021–2050	4(-9 – 18)	5(-12 – 23)	3(-10 – 16)	4(-7 – 15)	—	—	9.2
2070–2099	* 12(-4 – 28)	* 10(-3 – 23)	7(-8 – 21)	7(-2 – 15)	—	—	

REGION GRÖ

	GCM-A1FI	GCM-A2	GCM-B2	GCM-B1	RCMHAD-A2	RCMEXT-A2	INT.VAR
DEC-FEB							
2021–2050	* 9(-1 – 19)	* 9(1 – 16)	* 10(2 – 17)	* 8(0 – 16)	—	—	7.6
2070–2099	* 28(7 – 50)	* 24(12 – 37)	* 19(7 – 32)	* 16(8 – 24)	—	—	
MAR-MAY							
2021–2050	7(-7 – 20)	* 8(-2 – 18)	5(-7 – 17)	6(-8 – 19)	—	—	7.2
2070–2099	* 24(8 – 39)	* 18(8 – 29)	* 15(0 – 29)	* 11(0 – 23)	—	—	
JUN-AUG							
2021–2050	* 11(1 – 20)	* 9(-2 – 19)	* 11(3 – 18)	* 10(3 – 17)	—	—	6.7
2070–2099	* 29(8 – 51)	* 24(4 – 43)	* 16(4 – 27)	* 15(2 – 27)	—	—	
SEP-NOV							
2021–2050	* 9(2 – 16)	* 7(0 – 15)	* 7(0 – 14)	7(1 – 13)	—	—	6.9
2070–2099	* 26(16 – 36)	* 22(13 – 30)	* 16(8 – 24)	* 14(8 – 19)	—	—	

RAPORTTEJA — RAPPORTER — REPORTS

1986: 1. Savolainen, Anna Liisa et al., 1986. Radioaktiivisten aineiden kulkeutuminen Tshernobylin ydinvoimalaonnettomuuden aikana. Väliaikainen raportti. 39 s.

2. Savolainen, Anna Liisa et al., 1986. Dispersion of radioactive release following the Chernobyl nuclear power plant accident. Interim report. 44 p.

3. Ahti, Kari, 1986. Rakennussääpalvelukokeilu 1985-1986. Väliraportti Helsingin ympäristön talvikokeilusta 18.11.-13.3.1986. 26 s.

4. Korhonen, Ossi, 1986. Pintatuulen vertailumittauksia lentoasemilla. 38 s.

1987: 1. Karppinen, Ari et al., 1987. Description and application of a system for calculating radiation doses due to long range transport of radioactive releases. 50 p.

2. Venäläinen, Ari, 1987. Ilmastohavaintoihin perustuva arvio jyrsinturpeen tuotantoedellytyksistä Suomessa. 35 s.

3. Kukkonen, Jaakko ja Savolainen, Anna Liisa, 1987. Myrkyllisten kaasujen päästöt ja leviäminen onnettomuustilanteissa. 172 s.

4. Nordlund, Göran ja Rantakrans, Erkki, 1987. Matemaattisfysikaalisten ilmanlaadun arviointimallien luotettavuus. 29 s.

5. Ahti, Kari, 1987. Rakennussäätutkimuksen loppuraportti. 45 s.

6. Hakola, Hannele et al., 1987. Otsonin vaihteluista Suomessa yhden vuoden havaintoaineiston valossa. 64 s.

7. Tammelin, Bengt ja Erkiö, Eero, 1987. Energialaskennan säätiedot – suomalainen testivuosi. 108 s.

1988: 1. Eerola, Kalle, 1988. Havaintojen merkityksestä numeerisessa säänennustuksessa. 36 s.

2. Fredrikson, Liisa, 1988. Tunturisääprojekti 1986-1987. Loppuraportti. 31 s.

3. Salmi, Timo and Joffre, Sylvain, 1988. Airborne pollutant measurements over the Baltic Sea: meteorological interpretation. 55 p.

4. Hongisto, Marke, Wallin, Markku ja Kaila, Juhani, 1988. Rikkipäästöjen vähentämistoimenpiteiden taloudellisesti tehokas valinta. 80 s.

5. Elomaa, Esko et al., 1988. Ilmatieteen laitoksen automaattisten merisääasemien käyttövarmuuden parantaminen. 55 s.

6. Venäläinen, Ari ja Nordlund, Anneli, 1988. Kasvukauden ilmastotiedotteen sisältö ja käyttö. 63 s.

7. Nieminen, Rauno, 1988. Numeeristen paine- ja ja korkeuskenttäennusteiden objektiivinen verifiointisysteemi sekä sen antamia tuloksia vuosilta 1985 ja 1986. 35 s.

1989: 1. Ilvessalo, Pekko, 1989. Yksittäisestä piipusta ilmaan pääsevien epäpuhtauksien suurimpien tuntipitoisuuksien arviointimenetelmä. 21 s.

1992: 1. Mhita, M.S. and Venäläinen, Ari, 1991. The variability of rainfall in Tanzania. 32 p.

2. Anttila, Pia (toim.), 1992. Rikki- ja typpilaskeuman kehitys Suomessa 1980-1990. 28 s.

1993: 1. Hongisto, Marke ja Valtanen Kalevi, 1993. Rikin ja typen yhdisteiden kaukokulkeutumismallin kehittäminen HIRLAM-sääennustemallin yhteyteen. 49 s.

2. Karlsson, Vuokko, 1993. Kansalliset rikkidioksidin analyysivertailut 1979 - 1991. 27 s.

1994: 1. Komulainen, Marja-Leena, 1995. Myrsky Itämerellä 28.9.1994. Säätilan kehitys Pohjois-Itämerellä M/S Estonian onnettomuusyönä. 42 s.

2. Komulainen, Marja-Leena, 1995. The Baltic Sea Storm on 28.9.1994. An investigation into the weather situation which developed in the northern Baltic at the time of the accident to m/s Estonia. 42 p.

1995: 1. Aurela, Mika, 1995. Mikrometeorologiset vuomittausmenetelmät - sovelluksena otsonin mittaaminen suoralla menetelmällä. 88 s.

2. Valkonen, Esko, Mäkelä, Kari ja Rantakrans, Erkki, 1995. Liikenteen päästöjen leviäminen katukuilussa - AIG-mallin soveltuvuus maamme oloihin. 25 s.

3. Virkkula, Aki, Lättilä, Heikki ja Koskinen, Timo, 1995. Otsonin maanpintapitoisuuden mittaaminen UV-säteilyn absorbtiolla: DOAS-menetelmän vertailu suljettua näytteenottotilaa käyttävään menetelmään. 29 s.

4. Bremer, Pia, Ilvessalo, Pekko, Pohjola, Veijo, Saari, Helena ja Valtanen, Kalevi, 1995. Ilmanlaatuennusteiden ja -indeksin kehittäminen Helsingin Käpylässä suoritettujen mittausten perusteella. 81 s.

1996: 1. Saari, Helena, Salmi, Timo ja Kartastenpää, Raimo, 1996. Taajamien ilmanlaatu suhteessa uusiin ohjearvoihin. 98 s.

1997: 1. Solantie, Reijo, 1997. Keväthallojen alueellisista piirteistä ja vähän talvipakkastenkin. 28 s.

1998: 1 Paatero, Jussi, Hatakka, Juha and Viisanen, Yrjö, 1998. Concurrent measurements of airborne radon-222, lead-210 and beryllium-7 at the Pallas-Sodankylä GAW station, Northern Finland. 26 p.

2 Venäläinen, Ari ja Helminen, Jaakko, 1998. Maanteiden talvikunnossapidon sääindeksi. 47 s.

3 Kallio, Esa, Koskinen, Hannu ja Mälkki, Anssi, 1998. VII Suomen avaruustutkijoiden COSPAR-kokous, Tiivistelmät. 40 s.

4 Koskinen, H. and Pulkkinen, T., 1998. State of the art of space weather modelling and proposed ESA strategy. 66 p.

5 Venäläinen, Ari ja Tuomenvirta Heikki, 1998. Arvio ilmaston lämpenemisen vaikutuksesta teiden talvikunnossapidon kustannuksiin. 19 s.

1999: 1 Mälkki, Anssi, 1999. Near earth electron environment modelling tool user/software requirements document. 43 p.

2 Pulkkinen, Antti, 1999. Geomagneettisesti indusoituvat virrat Suomen maakaasuverkostossa. 46 s.

3 Venäläinen, Ari, 1999. Talven lämpötilan ja maanteiden suolauksen välinen riippuvuus Suomessa.16 s.

4 Koskinen, H., Eliasson, L., Holback, B., Andersson, L., Eriksson, A., Mälkki, A., Nordberg, O., Pulkkinen, T., Viljanen, A., Wahlund, J.-E., Wu, J.-G., 1999. Space weather and interactions with scacecraft : spee final report. 191 p.

2000: 1 Solantie, Reijo ja Drebs, Achim, 2000. Kauden 1961 - 1990 lämpöoloista kasvukautena alustan vaikutus huomioiden, 38 s.

2 Pulkkinen, Antti, Viljanen, Ari, Pirjola, Risto, and Bear working group, 2000. Large geomagnetically induced currents in the Finnish high-voltage power system. 99 p.

3 Solantie, R. ja Uusitalo, K., 2000. Patoturvallisuuden mitoitussadannat: Suomen suurimpien 1, 5 ja 14 vrk:n piste- ja aluesadantojen analysointi vuodet 1959 - 1998 kattavasta aineistosta. 77 s.

4 Tuomenvirta, Heikki, Uusitalo, Kimmo, Vehviläinen, Bertel, Carter, Timothy, 2000. Ilmastonmuutos, mitoitussadanta ja patoturvallisuus: arvio sadannan ja sen ääriarvojen sekä lämpötilan muutoksista Suomessa vuoteen 2100. 65 s.

5 Viljanen, Ari, Pirjola, Risto and Tuomi, Tapio, 2000. Abstracts of the URSI XXV national convention on radio science. 108 p.

6 Solantie, Reijo ja Drebs, Achim, 2000. Keskimääräinen vuoden ylin ja alin lämpötila Suomessa 1961 - 90. 31 s.

7 Korhonen, Kimmo, 2000. Geomagneettiset mallit ja IGRF-appletti. 85 s.

2001: 1 Koskinen, H., Tanskanen, E., Pirjola, R., Pulkkinen, A., Dyer, C., Rodgers, D., Cannon, P., Mandeville, J.-C. and Boscher, D., 2001. Space weather effects catalogue. 41 p.

2 Koskinen, H., Tanskanen, E., Pirjola, R., Pulkkinen, A., Dyer, C., Rodgers, D., Cannon, P., Mandeville, J.-C. and Boscher, D., 2001. Rationale for a european space weather programme. 53 p.

3 Paatero, J., Valkama, I., Makkonen, U., Laurén, M., Salminen, K., Raittila, J. and Viisanen, Y., 2001. Inorganic components of the ground-level air and meteorological parameters at Hyytiälä, Finland during the BIOFOR project 1998-1999. 48 p.

4 Solantie, Reijo, Drebs, Achim, 2001. Maps of daily and monthly minimum temperatures in Finland for June, July, and August 1961-1990, considering the effect of the underlying surface. 28 p.

5 Sahlgren, Vesa, 2001. Tuulikentän alueellisesta vaihtelusta Längelmävesi-Roine -järvialueella. 33 s.

6 Tammelin, Bengt, Heimo, Alain, Leroy, Michel, Rast, Jacques and Säntti, Kristiina, 2001. Meteorological measurements under icing conditions : EUMETNET SWS II project. 52 p.

2002: 1 Solantie, Reijo, Drebs, Achim, Kaukoranta, Juho-Pekka, 2002. Lämpötiloja eri vuodenaikoina ja eri maastotyypeissä Alajärven Möksyssä. 57 s.

2. Tammelin, Bengt, Forsius, John, Jylhä, Kirsti, Järvinen, Pekka, Koskela, Jaakko, Tuomenvirta, Heikki, Turunen, Merja A., Vehviläinen, Bertel, Venäläinen, Ari, 2002. Ilmastonmuutoksen vaikutuksia energiantuotantoon ja lämmitysenergian tarpeeseen. 121 s.

2003: 1. Vajda, Andrea and Venäläinen, Ari, 2003. Small-scale spatial variation of climate in northern Finland. 34 p.

2. Solantie, Reijo, 2003. On definition of ecoclimatic zones in Finland. 44 p.

3. Pulkkinen, T.I., 2003. Chapman conference on physics and modelling of the inner magnetosphere Helsinki, Finland, August 25 -29, 2003. Book of abstracts. 110 p.

4. Pulkkinen, T. I., 2003. Chapman conference on physics and modelling of the inner magnetosphere Helsinki, Finland, August 25 -29, 2003. Conference program. 16 p.

5. Merikallio, Sini, 2003. Available solar energy on the dusty Martian atmosphere and surface. 84 p.

6. Solantie, Reijo, 2003. Regular diurnal temperature variation in the Southern and Middle boreal zones in Finland in relation to the production of sensible heat. 63 p.

2004: 1. Solantie, Reijo, Drebs, Achim and Kaukoranta, Juho-Pekka, 2004. Regular diurnal temperature variation in various landtypes in the Möksy experimental field in summer 2002, in relation to the production of sensible heat. 69 p.

2. Toivanen, Petri, Janhunen, Pekka and Koskinen, Hannu, 2004. Magnetospheric propulsion (eMPii). Final report issue 1.3. 78 p.

3. Tammelin, Bengt et al., 2004. Improvements of severe weather measurements and sensors – EUMETNET SWS II project. 101 p.

4. Nevanlinna, Heikki, 2004. Auringon aktiivisuus ja maapallon lämpötilan vaihtelut 1856 - 2003. 43 s.

5. Ganushkina, Natalia and Pulkkinen, Tuija, 2004. Substorms-7: Proceedings of the 7th International Confrence on Substorms. 235 p.

6. Venäläinen, Ari, Sarkkula, Seppo, Wiljander, Mats, Heikkinen, Jyrki, Ervasto, Erkki, Poussu, Teemu ja Storås, Roger, 2004. Espoon kaupungin talvikunnossapidon sääindeksi. 17 s.

7. Paatero, Jussi and Holmen, Kim (eds.), 2004. The First Ny-Ålesund - Pallas-Sodankylä atmospheric research workshop, Pallas, Finland 1 - 3 March 2004 - Extended abstracts. 61 p.

8. Holopainen, Jari, 2004. Turun varhainen ilmastollinen havaintosarja. 59 s.

2005: 1. Ruuhela, Reija, Ruotsalainen, Johanna, Kangas, Markku, Aschan, Carita, Rajamäki, Erkki, Hirvonen, Mikko ja Mannelin, Tarmo, 2005. Kelimallin kehittäminen talvijalankulun turvallisuuden parantamiseksi. 47 s.

2. Laurila, Tuomas, Lohila, Annalea, Tuovinen, Juha-Pekka, Hatakka, Juha, Aurela, Mika, Thum, Tea, Walden, Jari, Kuronen, Pirjo, Talka, Markus, Pesonen, Risto, Pihlatie, Mari, Rinne, Janne, Vesala, Timo, Ettala, Matti, 2005. Kaatopaikkojen kaasupäästöjen ja haihdunnan mikrometeorologisten mittausmenetelmien kehittäminen (MIKROMETKAA). Tekesin Streams – ohjelman hankken loppuraportti. 34 s.

3. Siili, Tero, Huttunen, Emilia, Koskinen, Hannu ja Toivanen, Petri (toim.), 2005. Kymmenes Suomen avaruustutkijoiden kokous (FinCospar) Kokousjulkaisu. 57 s.

4. Solantie, Reijo and Pirinen, Pentti, 2005. Diurnal temperature variation in inversion situations. 34 s.

5. Venäläinen, Ari, Tuomenvirta, Heikki, Pirinen, Pentti and Drebs, Achim, 2005. A basic Finnish climate data set 1961 – 2000 – description and illustrations. 24 p.

6. Tammelin, Bengt, Säntti, Kristiina, Dobech, Hartwig, Durstewich, Michel, Ganander, Hans, Kury, Georg, Laakso, Timo, Peltola, Esa, Ronsten, Göran, 2005. Wind turbines in icing environment: improvement of tools for siting, certification and operation – NEW ICETOOLS. 127 p.

2006: 1. Mälkki, Anssi, Kauristie, Kirsti and Viljanen Ari, 2006. Auroras Now! Final Report, Volume I. 73 p.

2. Pajunpää, K. and Nevanlinna, H. (eds.), 2006. Nurmijärvi Geophysical Observatory : Magnetic results 2003. 47 p.

3. Pajunpää, K. and Nevanlinna, H. (eds.), 2006. Nurmijärvi Geophysical Observatory : Magnetic results 2004. 47 p.

4. Pajunpää, K. and Nevanlinna, H. (eds.), 2006. Nurmijärvi Geophysical Observatory : Magnetic results 2005. 49 p.

5. Viljanen, A. (toim.), 2006. Sähkömagnetiikka 2006. Tiivistelmät – Abstracts. 30 s.

6. Tuomi, Tapio J.& Mäkelä, Antti, 2006. Salamahavainnot 2005 - Lightning observations in Finland, 2006. 39 p.

7. Merikallio, Sini, 2006. Preliminary report of the analysis and visualisation software for SMART-1 SPEDE and EPDP instruments, 70 p.

8. Solantie, Reijo, Pirinen, Pentti, 2006. Orografian huomioiminen loka-huhtikuun sademäärien alueellisissa analyyseissä, 34 s.

9. Ruosteenoja, Kimmo, Jylhä, Kirsti, Räisänen, Petri, 2006. Climate projections for the Nordic CE project – an analysis of an extended set of global regional climate model runs, 28 p.

Ilmatieteen laitos
Erik Palménin aukio 1, Helsinki
tel. (09) 19 291
www.fmi.fi

ISBN 951-697-659-X
ISSN 0782-6079
Yliopistopaino
Helsinki